Molecular Pharmacology Fast Forward. Published on October 12, 2012 as doi:10.1124/mol.112.082651

The biarylpyrazole compound AM251 alters mitochondrial physiology via proteolytic degradation of ERRα.

Susan M. Krzysik-Walker, Isabel González-Mariscal, Morten Scheibye-Knudsen, Fred E. Indig, and Michel Bernier

Laboratory of Clinical Investigation (S.M.K.-W., I.G.-M., F.E.I., M.B.), Laboratory of Molecular Gerontology (M.S.-K.), National Institute on Aging, National Institutes of Health, Baltimore, MD

Molecular Pharmacology Fast Forward. Published on October 12, 2012 as DOI: 10.1124/mol.112.082651
This article has not been copyedited and formatted. The final version may differ from this version.

Running Title: Proteasomal degradation of ERRα by AM251

Corresponding Author: Michel Bernier, Ph.D. Laboratory of Clinical Investigation, National Institute on Aging, NIH, Biomedical Research Center, 251 Bayview Boulevard, Suite 100, Baltimore, Maryland 21224, USA. Phone: 410-558-8199; Fax: 410-558-8381; Email: Bernierm@mail.nih.gov

Text pages: 30
Total Figures: 5
Tables: 0
References: 46

Abstract: 224 words
Introduction: 597 words
Discussion: 1331 words

ABBREVIATIONS: AM251, 1-(2,4-dichlorophenyl)-5-(4-iodophenyl)-4-methyl-N-1-piperidinyl-1H-pyrazole-3-carboxamide; CHX, cycloheximide; ERR, estrogen-related receptor; ERRE, ERR-responsive element; PGC-1, peroxisome proliferator-activated receptor γ coactivator-1; PMA, phorbol 12-myristate 13-acetate; rimonabant (SR141716A), 5-(4-chlorophenyl)-1-(2,4-dichloro-phenyl)-4-methyl-*N*-(piperidin-1-yl)-1*H*-pyrazole-3-carboxamide; RT-PCR, real-time polymerase chain reaction; siRNA, small interfering RNA; SLV319 (Ibipinabant), 3-(4-chlorophenyl)-N-[(4-chlorophenyl)sulfonyl]-4,5-dihydro-N'-methyl-4-phenyl-1H-pyrazole-1-carboximidamide; XCT790, thiadiazoleacrylamide; $\Delta\psi_m$, mitochondrial membrane potential;

Molecular Pharmacology Fast Forward. Published on October 12, 2012 as DOI: 10.1124/mol.112.082651
This article has not been copyedited and formatted. The final version may differ from this version.

ABSTRACT

The orphan nuclear receptor estrogen-related receptor alpha (ERRα) directs the transcription of nuclear genes involved in energy homeostasis control and the regulation of mitochondrial mass and function. A crucial role for controlling ERRα-mediated target gene expression has been ascribed to the biarylpyrazole compound, AM251, through direct binding to and destabilization of ERRα protein. Here, we provide evidence that structurally-related AM251 analogs also have negative impacts on ERRα protein levels in a cell type-dependent manner, while having no deleterious actions on ERRγ. We show that these off-target cellular effects of AM251 are mediated by proteasomal degradation of nuclear ERRα. Cell treatment with the nuclear export inhibitor, leptomycin B, did not prevent AM251-induced destabilization of ERRα protein, whereas proteasome inhibition with MG132 stabilized and maintained its DNA-binding function, indicative of ERRα being a target of nuclear proteasomal complexes. NativePAGE analysis revealed that ERRα formed a ~220 kDa multiprotein nuclear complex that was devoid of ERRγ and the coregulator peroxisome proliferator-activated receptor γ coactivator-1. AM251 induced SUMO-2,3 incorporation in ERRα in conjunction with increased protein kinase C activity, whose activation by phorbol ester also promoted ERRα protein loss. Downregulation of ERRα by AM251 or small interfering RNA led to increased mitochondria biogenesis while negatively impacting mitochondrial membrane potential. These results reveal a novel molecular mechanism by which AM251 and related compounds alter mitochondrial physiology through destabilization of ERRα.

Molecular Pharmacology Fast Forward. Published on October 12, 2012 as DOI: 10.1124/mol.112.082651
This article has not been copyedited and formatted. The final version may differ from this version.

Introduction

The biarylpyrazole class of cannabinoid 1 receptor (CB_1R) inverse agonists, which includes AM251 and rimonabant (SR141716A), has therapeutic potential as animal and clinical data suggest that they mediate suppression of appetite and improve glucose homeostasis (Padwal and Majumdar, 2007). However, administration of rimonabant still stimulates neurogenesis and induces cannabinoid-like effects in mice deficient in cannabinoid 1 receptors (Jin et al., 2004; Wiley et al., 2012), indicating the involvement of additional targets. Indeed, the neuroprotective effect of rimonabant requires the vanilloid receptor VR1, independent of the CB_1R interaction (Jin et al., 2004; Pegorini et al., 2006). These biarylpyrazole compounds also appear to have targets other than CB_1R, CB_2R, and VR1 (Raffa and Ward, 2012); for example, AM251 and rimonabant are agonists of GPR55, a recently deorphanized G-protein coupled receptor that is expressed in peripheral tissues and is positively associated with obesity in human (Moreno-Navarrete et al., 2012). However, the effect of these compounds on the cellular functions of GPR55 requires low micromolar concentrations. For instance, AM251 induces sustained and oscillatory Ca^{2+} responses reminiscent of responses triggered by the endogenous GPR55 ligand, lysophosphatidylinositol, using a maximally effective concentration of AM251 (3 μM), with an EC_{50} of 612 ± 86 nM (Henstridge et al., 2009). Moreover, the redistribution of β-arrestin 2 in U2OS cells containing GPR55 is visualized after treatment with 30 μM rimonabant and 30 μM AM251 (Kapur et al., 2009). Lastly, 1-10 μM of rimonabant and AM251 are used to demonstrate the involvement of GPR55 in cannabinoid-triggered calcium signaling in endothelial cells (Waldeck-Weiermair et al., 2008).

Our recent study has revealed that the cellular responses to AM251 (5 μM) relied on the binding to and destabilization of estrogen-related receptor alpha (ERRα) protein (Fiori et al., 2011). Importantly, mice lacking ERRα exhibit reduced fat mass and were resistant to diet-induced obesity (Luo et al., 2003), a phenotype similar to that of mice lacking CB_1R (Ravinet Trillou et al., 2004). Members of the ERR subfamily, which encompass ERRα, ERRβ and ERRγ, are constitutively active and do not require

specific ligands for transcriptional activity (Ariazi and Jordan, 2006). The orphan hormone nuclear receptor ERRα binds to promoter sites of target genes as dimers (Horard et al., 2004). The binding of ERRα to estrogen-response element (ERE) or ERR-response element (ERRE) on specific DNA target sites leads to either transcriptional activation or repression partly depending on the presence of coregulators (Ariazi and Jordan, 2006). A number of nuclear receptor coactivators, including the peroxisome proliferator-activated receptor γ coactivator-1 (PGC-1) α and β, interact with ERRα and potentiate its transcriptional activity (Zhang and Teng, 2000; Xie et al., 1999). The recent report of the crystal structure of the ERRα ligand-binding domain in complex with PGC-1α has provided new evidence for ligand-independent transcriptional activation of ERRα (Kallen et al., 2004). PGC-1α and ERRα work in concert to promote regulation of genes that control key aspects of metabolism including mitochondrial biogenesis (Schreiber et al., 2004; Eichner and Giguère, 2011).

It is therefore possible that alterations in ERRα levels may be responsible for some of the off-target effects of AM251 that led to the upregulation of epidermal growth factor receptor expression and signaling (Fiori et al., 2011). Here, we investigated the molecular mechanisms involved in the regulation of ERRα protein stability by AM251. Moreover, because of the important role of ERRα in the control of cellular metabolism, we also sought to determine if AM251 treatment resulted in altered mitochondrial biogenesis and function through destabilization of this orphan nuclear receptor. Our findings provide novel mechanistic insights into inducible posttranslational modifications of ERRα that subsequently augment mitochondrial mass but reduce mitochondrial bioenergetic functions.

Molecular Pharmacology Fast Forward. Published on October 12, 2012 as DOI: 10.1124/mol.112.082651
This article has not been copyedited and formatted. The final version may differ from this version.

Materials and Methods

Chemicals. AM251 was purchased from Cayman Chemical (Ann Arbor, MI). Ammonium chloride, cycloheximide, leptomycin B, MG132, XCT790 and phorbol 12-myristate 13-acetate (PMA) were purchased from Sigma-Aldrich (St-Louis, MO). Leupeptin was purchased from Fischer Scientific (Pittsburgh, PA), while rimonabant and SLV-319 were obtained from J. F. McElroy (Jenrin Discovery, Inc. West Chester, PA).

Cell Culture and Treatments. Human PANC-1 cells (ATCC, Manassas, VA) were cultured in phenol red-free Dulbecco's modified Eagle's medium (DMEM) supplemented with 4.5 g/L D-glucose, 4 mM glutamine, 1 mM pyruvate, 1.5 g/L sodium bicarbonate, 10% heat-inactivated fetal bovine serum (FBS; HyClone, Logan, UT), and penicillin/streptomycin. Human ES-2 cells were cultured in McCoy's 5A medium supplemented with 1 mM pyruvate, 1.5 mM glutamine, 0.1 mM non-essential amino acids, 1.5 g/L sodium bicarbonate, 10% heat-inactivated FBS and penicillin/streptomycin. Human HepG2 cells were cultured in Minimum Essential medium supplemented with 4 mM glutamine, 1 mM pyruvate, 1.5 g/L sodium bicarbonate, 10% heat-inactivated FBS and penicillin/streptomycin. All cell lines were maintained at 37^{o}C with 5% CO_2, and medium replaced every 2-3 days. Unless otherwise indicated, cells were rinsed twice with phosphate-buffered saline (PBS) and serum starvation was performed for 3 h before treatment began.

RNA Extraction, cDNA Synthesis and Quantitative PCR. Following treatments, cells were washed twice with ice-cold PBS and snap frozen in liquid nitrogen. RNA was extracted using an RNeasy Mini kit (Qiagen, Valencia, CA) and 1 µg RNA was reverse transcribed using qScript cDNA SuperMix (Quanta Biosciences, Gaithersburg, MD) according to the manufacturer's instructions. Gene expression was quantified and analyzed using quantitative PCR as described previously (Fiori et al., 2011).

Small Interfering RNA for ERRα. Small interfering RNAs targeting ERRα were purchased from Qiagen and contained the following sequences: ERRα siRNA: [forward 5'-GAGAGAUUGUGGUC-

Molecular Pharmacology Fast Forward. Published on October 12, 2012 as DOI: 10.1124/mol.112.082651
This article has not been copyedited and formatted. The final version may differ from this version.

ACCAUTT-3'; reverse 5'-AUGGUGACCACAAUCUCUCGG-3'] and negative control siRNA: [forward 5'-UUCUCCGAACGUGUCACGUdTdT-3'; reverse 5'-ACGUGACACGUU-CGGAGAAdTdT-3']. These siRNAs have been validated to perform efficient knockdown with minimal off-target effects (Fiori et al., 2011). PANC-1 cells were reverse transcribed using Lipofectamine RNAiMAX reagent (Invitrogen, Carlsbad, CA) according to the manufacturer's instructions. Briefly, for each well of a 4-well chamber slide (Lab-Tek; Nunc, Rochester, NY), the RNAi duplex-Lipofectamine RNAiMAX complex was prepared using 0.1 nmoles of siRNA duplex and 1 µl of Lipofectamine RNAiMAX in 100 µL Opti-MEM I medium and incubated for 15 min at room temperature. PANC-1 cells (40,000 cells/well) in complete growth medium without antibiotics were then plated into chambers and incubated for 48 h prior to use. Knockdown efficiency was determined by Western blot analyses. Three independent transfection experiments were performed.

Subcellular Fractionation. Fractionation of cytoplasmic and nuclear protein extracts was carried out using NE-PER™ nuclear and cytoplasmic extraction reagents (Thermo Scientific, Rockford, IL) supplemented with 1 mM sodium orthovanadate, protease inhibitor cocktail set I and phosphatase inhibitor cocktail set II (Calbiochem-EMB, San Diego, CA). Mitochondrial and cytosolic fractions were isolated using the mitochondria isolation kit for cultured cells (MitoSciences Inc., Eugene, OR) following the manufacturer's protocol. The cytosolic fractions were concentrated using Microcon YM-3 concentrators (Millipore-Amicon, Billerica, MA).

Immunoprecipitation. Following treatments, cells were washed twice with ice-cold PBS and snap frozen in liquid nitrogen. Cells were lysed and nuclear extracts were prepared as described above. Equal amounts of nuclear extracts were diluted in radioimmune precipitation assay (RIPA) buffer (25 mM HEPES, 134 mM NaCl, 1% NP-40, 0.1% SDS, 1 mM sodium orthovanadate, 0.5% sodium deoxycholate, 100 mM NaF) supplemented with phosphatase and protease inhibitor cocktails, and precleared with protein G agarose beads (50% v/v, cat. No. 16-266, Millipore). Immunoprecipitation was carried out using a 1:40 dilution of either ERRα (cat. No. ab76228) or SUMO-2,3 (cat. No. ab3742) (Abcam,

Molecular Pharmacology Fast Forward. Published on October 12, 2012 as DOI: 10.1124/mol.112.082651
This article has not been copyedited and formatted. The final version may differ from this version.

Cambridge, MA) overnight at 4°C, followed by incubation with protein G-agarose for 3 h at 4°C. As a negative control, nuclear extracts were incubated with protein G beads alone. The resin was then centrifuged at 6000 x g for 30 sec and washed 3 times in RIPA and twice in 50 mM HEPES, pH 7.4, containing 0.1% Triton X-100. Bound proteins were eluted in 2X Laemmli sample buffer and resolved by SDS-PAGE followed by Western blotting with the anti-SUMO-2,3 or anti-ERRα antibodies.

DNA-binding Activity of ERRα. The protein content in PANC-1 nuclear extracts was quantified using the bicinchoninic acid assay kit (Thermo Scientific). Protein-DNA binding activity was assessed using a streptavidin-agarose pulldown assay as previously described (Wu, 2006). Briefly, one hundred fifty μg of nuclear extracts were incubated with 1.5 μg biotinylated oligonucleotide duplex and 10 μL streptavidin agarose beads (Vector Laboratories, Burlingame, CA) in 200 μL PBS supplemented with 1 mM sodium orthovanadate and protease and phosphatase inhibitor cocktails. The biotinylated double-stranded oligonucleotides contained either the wild-type ERRE binding motif (5'-biotin-AGGTCACAGTGACCTAGGTCACAGTGACCTAGGT-3' and 5'-biotin-ACCTAGGTCACTGTGACCTAGGTCACTGTGACCT-3') or an ERRE mutant oligonucleotide (5'-biotin-AGTACACATAGACCTAGTACACATAGACCTAGTA-3' and 5'-biotin-TACTAGGTCTATGTGTACTAGGTCTATGTGTACT-3') (Integrated DNA Technologies, Inc., Coralville, IA). Following 2 h incubation at room temperature, the complexes were sedimented by centrifugation at 550 x g for 1 min at 4°C, washed three times with PBS and eluted in Laemmli sample buffer. Proteins were resolved by SDS-PAGE and analyzed by Western blot.

Gel Electrophoresis and Western Blot Analysis. Unless otherwise noted, total cell extracts were prepared by lysing cells in ice-cold RIPA buffer supplemented with 1 mM sodium orthovanadate, phosphatase and protease inhibitor cocktails for 20 min on ice with occasional vortexing. Following centrifugation at 12000 x g for 15 min at 4°C to remove insoluble material, lysates were collected and protein quantified using the bicinchoninic acid assay kit. To perform traditional denatured SDS-PAGE analyses, protein extracts were prepared with Laemmli sample buffer and resolved on Novex® 4-12%

Molecular Pharmacology Fast Forward. Published on October 12, 2012 as DOI: 10.1124/mol.112.082651
This article has not been copyedited and formatted. The final version may differ from this version.

Tris-glycine gels (Invitrogen) under reducing conditions. For blue native gel electrophoresis, samples were prepared using the NativePAGE Sample Buffer and G-250 Sample Additive (Invitrogen), and were resolved on Novex® NativePAGE 4-16% Bis-Tris gels (Invitrogen), according to the manufacturer's instructions. Proteins were then transferred to polyvinylidene difluoride membranes using the iBLOT apparatus (Life Technologies). Rabbit polyclonal antibodies generated against ERRα (ab76228), ERRγ (ab49129), SUMO-2,3 (ab3742), and VDAC1/Porin (ab15895) were purchased from Abcam. Rabbit polyclonal antibodies against PGC-1 (sc-13067) and cytochrome c (H-104), and monoclonal antibodies against Hsp70 (sc-32239) and GAPDH (sc-32233) were from Santa Cruz Biotechnology, Inc. (Santa Cruz, CA). Monoclonal antibodies against complex II subunit 70 kDa (MS204/C582) and complex III subunit core 2 (MS304) were from Mitosciences, Inc., while monoclonal anti-Hsp90 (cat. No. 610419) was from BD Transduction Laboratories (Sparks, MD). Rabbit polyclonal anti-phosphorylated MARCKS (cat. No. 2741) was purchased from Cell Signaling Technology, Inc. (Danvers, MA). Unless otherwise indicated, a dilution of 1:1000 was used for all primary antibodies. The immobilized primary antibodies were visualized after incubation with horseradish peroxidase-conjugated secondary antibodies (GE Healthcare, Piscataway, NJ) and enhanced chemiluminescence with ECL or ECL Plus reagents (GE Healthcare). The quantitation of the immunoreactive bands was performed by volume densitometry using ImageJ software (NIH, Bethesda, MD).

Immunofluorescence Microscopy. Cells were seeded at 5 x 10^4 cells/well in complete medium into chamber slides (Nunc). Forty-eight h later, cells were maintained in serum-free medium for 3-4 h and then incubated as indicated in the text. After completion of treatments, medium was replaced with serum-free medium containing 100 nM MitoTracker Red CMXRos (Invitrogen-Molecular Probes, Eugene, OR) for 10 min at 37^{o}C, after which cells were rinsed in PBS, fixed with 4% paraformaldehyde for 20 min and then permeabilized for 5 min in 0.3% Triton-X100/0.1% BSA in PBS. After a blocking step (5% BSA in PBS), cells were incubated with rabbit anti-ERRα antibody overnight at 4ºC, followed by incubation with AlexaFluor 488-conjugated goat anti-rabbit IgG (Invitrogen). Cells were mounted in Prolong Gold

Molecular Pharmacology Fast Forward. Published on October 12, 2012 as DOI: 10.1124/mol.112.082651
This article has not been copyedited and formatted. The final version may differ from this version.

antifade reagent containing 4',6-diamidino-2-phenylindole (Invitrogen) and analyzed by confocal microscopy using a Zeiss LSM 710 microscope (Thornwood, NY). Images were processed using the Zeiss Zen software.

Measurement of Mitochondrial Mass and Mitochondrial Membrane Potential ($\Delta\psi_m$). Mitochondrial mass was measured by Mitotracker Green FM (20 nM, cat. No. M-7514, Invitrogen) staining. Mitochondrial membrane potential ($\Delta\psi_m$) was measured with the fluorescent lipophilic cationic dye, tetramethylrhodamine methylester (TMRM; 20 nM, cat. No. T-668, Invitrogen), that accumulates within mitochondria according to the $\Delta\psi_m$. Following treatment with AM251 (5 μM) or XCT790 (2.5 μM) for 16 h, cells were stained either with Mitotracker Green FM or TMRM for 15 min at 37^{o}C, and fluorescence was measured by flow cytometry using the BD Accuri C6 flow cytometer (Accuri Cytometers, Ann Arbor, MI). In each analysis, 10,000 events were recorded and FL-1 (Mitotracker green) and FL-2 (TMRM) fluorescence was obtained after gating for live cells.

Statistical Analysis. Results are represented as means ± SEM unless otherwise specified. Data were analyzed using KaleidaGraph software (Version 4.1, Synergy Software, Reading, PA). Statistical analyses were performed using either a Student's *t* test for unpaired data or ANOVA with Fisher's LSD post-hoc test analysis. A probability level of $P < 0.05$ was considered statistically significant.

Molecular Pharmacology Fast Forward. Published on October 12, 2012 as DOI: 10.1124/mol.112.082651
This article has not been copyedited and formatted. The final version may differ from this version.

Results

The Biarylpyrazole Class of Compounds Destabilize ERRα Protein. Our previous study has shown that AM251 down-regulates the expression of ERRα protein in PANC-1 cells (Fiori et al., 2011), and an independent study has reported that the selective ERRα inverse agonist, XCT790, induces the degradation of ERRα (Lanvin et al., 2007). We compared the effects of other compounds that are structurally related to AM251, specifically rimonabant and SLV319, in term of potency toward regulation of ERRα protein levels. A 16-h treatment of PANC-1 cells with maximal concentration (5 μM) of AM251, rimonabant, and SLV319 significantly decreased the levels of ERRα protein by ~60-70% ($P < 0.001$), whereas the effect was maximal (~95% reduction) with XCT790 (Fig. 1A). Incubation of PANC-1 cells with increasing concentrations of AM251 and related compounds produced a dose-dependent reduction in ERRα levels, with an IC_{50} ranging from 0.7 -1 μM (Fig. 1B).

Two other cell lines were also tested for their sensitivity to the biarylpyrazole compounds. While ES-2 and HepG2 cells were very responsive to XCT790, HepG2 cells showed refractoriness to the suppressive action of AM251, rimonabant and SLV319 (Supplemental Fig. 1A and B). In contrast, the sensitivity of ES-2 cells to these compounds was reminiscent of PANC-1 cells. Under these experimental conditions, the levels of ERRγ were unaffected by the biarylpyrazole compounds or XCT790 (Fig. 1A, Supplemental Fig. 1). These data suggest that the effect of AM251 and related analogs on the accumulation of ERRα protein is cell type-dependent.

AM251-mediated Proteasomal Degradation of ERRα. The half-life of ERRα protein was determined by treating PANC-1 cells either with the protein synthesis inhibitor, cycloheximide (CHX, 10 μg/ml), or AM251 in a time-course experiment. Immunoblot analysis of total cell lysates showed rapid degradation rate of ERRα by CHX, with a $t_{1/2}$ of 5 h (Fig. 2A). However, the half-life of ERRα protein was ~10 h following AM251 treatment, suggesting confounding contributions from transcription and/or translation. Neither PGC-1 nor GAPDH protein expression was altered by these treatments. To assess

Molecular Pharmacology Fast Forward. Published on October 12, 2012 as DOI: 10.1124/mol.112.082651
This article has not been copyedited and formatted. The final version may differ from this version.

whether the destabilization of ERRα in response to AM251 stemmed from proteasomal degradation, PANC-1 cells were pretreated with the proteasome inhibitor, MG132, for 1 h followed by the addition of AM251 for 6 h (Fig. 2B). The results show complete suppression in ERRα protein degradation in MG132-treated cells, indicating that proteasome activity is likely to play a key role in the AM251-mediated destabilization of this orphan nuclear receptor.

To assess the effect of AM251 on the localization of ERRα, nuclear and cytosolic fractions were isolated and subjected to Western blot analysis. As shown in Fig. 2C, ERRα was found predominantly in the nuclear fraction, although a significant amount was detected in the extranuclear compartment as well. Treatment with AM251 caused a decrease in ERRα levels in both subcellular fractions; however, inhibition of the proteasome complex with MG132 completely prevented the loss or redistribution of ERRα upon AM251 treatment (Fig. 2C, *upper panel*). Analysis of BRG-1 and IκBα as markers of nuclear and cytosolic proteins, respectively, confirmed the absence of cross-contamination during the subcellular fractionation process (Fig. 2C, *lower panel*).

DNA-binding Properties of the ERRα-containing Multiprotein Complexes. We determined if AM251 altered the DNA-binding property of ERRα. It has been previously reported that ERRα can bind to estrogen-response elements (ERE) containing the recognition motif AGGTCAnnnTGACCT and that ERRα also recognizes the single consensus half-site sequence TNAAGGTCA, referred to as an ERR-response element (ERRE) (Sladek et al., 1997). Here, a DNA affinity immunoprecipitation assay was used to assess the binding of ERRα to the agarose-conjugated ERRE consensus or mutated recognition sequences. The assay combines an affinity step with Western blot analysis to detect the DNA-bound ERRα (Wu, 2006). In the absence of MG132, the level of binding of ERRα to its target DNA was markedly reduced upon treatment of PANC-1 cells with AM251 or XCT790, as compared to control cells (Fig. 3A, lanes 4 and 6 *vs.* 2). In contrast, treatment with MG132 alone clearly increased the amount of DNA-bound ERRα and conferred protection against alteration in the DNA binding capacity of ERRα elicited by AM251 and XCT790 (Fig. 3A, lanes 5 and 7 *vs.* 3). The oligonucleotide dimer with mutated

Molecular Pharmacology Fast Forward. Published on October 12, 2012 as DOI: 10.1124/mol.112.082651
This article has not been copyedited and formatted. The final version may differ from this version.

ERRE recognition sequence bound poorly with ERRα (Fig. 3A, lane 1 *vs*. 2). These results suggest that inhibition of the proteasome complex canceled the detrimental effects of AM251 and XCT790 on the DNA-binding capacity of ERRα.

The orphan nuclear receptor ERRα interacts with a number of binding partners for full transcriptional activity. We analyzed ERRα-containing multi-protein complexes using NativePAGE gels, a technique that offers a higher resolution than gel filtration or sucrose density ultracentrifugation (Swamy et al., 2006). Western blotting of the nuclear extract from untreated PANC-1 cells showed a stable ERRα-containing multiprotein complex of ~220 kDa, whose relative abundance increased in MG132-treated cells (Fig. 3B, lane 2 *vs*. 1). Consistent with the DNA pull-down experiment, the abundance of the complex was markedly lower in PANC-1 cells treated with AM251 and XCT790 in the absence of MG132; however, inhibition of the proteasome caused a marked accumulation of the 220-kDa species (Fig. 3B, lanes 3 and 5 *vs*. 4 and 6). No free monomeric or dimeric forms of ERRα were observed by these treatments. Immunoblot analysis of duplicate membranes demonstrated that the 220-kDa complex was devoid of known ERRα-interacting proteins, including ERRγ and the coregulators PGC-1 and RIP140 (Fig. 3C).

Nuclear ERRα as a Putative Target for Phosphorylation-mediated SUMOylation in Response to AM251. Because ERRα could be interacting with components of the proteasome in both the nuclear and cytosolic compartments, PANC-1 cells were pretreated with the nuclear export inhibitor, leptomycin B, alone or together with MG132, followed by subsequent incubation with AM251 or XCT790. As shown in Fig. 4A, leptomycin alone did not confer protection whereas the combination leptomycin plus MG132 prevented ERRα degradation induced by AM251 and XCT790. These results indicate that nuclear proteolytic activity may be responsible for the destabilization of ERRα.

Since proteasome inhibition results in impaired degradation of ERRα by AM251, we tested directly whether ERRα is a SUMOylation target. SUMOylation is a known posttranslational modification of ERRα (Tremblay et al, 2008), and functions as a signal for proteasomal degradation (Miteva et al, 2010).

Molecular Pharmacology Fast Forward. Published on October 12, 2012 as DOI: 10.1124/mol.112.082651
This article has not been copyedited and formatted. The final version may differ from this version.

Here, anti-ERRα immunoprecipitates from nuclear fractions were analyzed by immunoblotting with anti-SUMO-2,3 antibody, and showed inducible SUMOylation of ERRα in cells stimulated with AM251 (Fig. 4B, *upper panel*). A reciprocal experiment was performed, whereby anti-SUMO-2,3 immunoprecipitates were immunoblotted with ERRα antibody and gave similar results (Fig. 4B, *second panel*). No signal was observed in the immunoprecipitation control with protein G beads alone.

Phosphorylation has been shown to be a requirement for ERRα SUMOylation (Tremblay et al., 2008; Vu et al., 2007), with protein kinase Cδ being one of the potential kinases involved (Barry and Giguère, 2005). Similar to AM251, activation of PKC with the phorbol ester PMA resulted in a significant reduction in ERRα protein levels (Fig. 4C) in the absence of detectable alteration in ERRα mRNA expression (Fig. 4D). Moreover, both AM251 and PMA elicited rapid and significant phosphorylation of a major PKC substrate, **M**yristoylated **A**lanine-**R**ich **C**-**K**inase **S**ubstrate (MARCKS) (Fig. 4E). These data indicate that PKC-dependent phosphorylation may be a prerequisite for AM251-mediated SUMOylation and proteolytic degradation of ERRα.

ERRα Degradation Alters the Number of Mitochondria and Mitochondrial Membrane Potential. Through transcriptional regulation of respiratory gene expression, ERRα controls the energy generating functions of mitochondria (Eichner and Giguere, 2011). Interestingly, AM251-treated PANC-1 cells exhibited a sharp reduction in MitoTracker Red CMXRos staining, which is dependent upon mitochondrial membrane potential (Fig. 5A). In support of this finding, downregulation of ERRα expression by siRNA led to a marked reduction in MitoTracker Red CMXRos staining, as compared to cells transfected with control siRNA (Fig. 5B). Consistent with the refractoriness of HepG2 cells to AM251-dependent reduction in ERRα protein levels, the mitochondrial membrane potential remained unaffected by AM251 treatment in these cells (Supplemental Fig. 2).

Mitotracker Green is a probe used to evaluate the mitochondrial mass and differentiate intact mitochondria from cellular debris while the measure of $\Delta\psi_m$, monitored by the fluorescence of mitochondrially-loaded cationic potentiometric dye TMRM, serves to measure the electrical gradient

Molecular Pharmacology Fast Forward. Published on October 12, 2012 as DOI: 10.1124/mol.112.082651
This article has not been copyedited and formatted. The final version may differ from this version.

across the mitochondria inner membrane established by electron transport chain activity (Seppet et al., 2009). Flow cytometric analyzes of Mitotracker Green and TMRM fluorescence profiles were performed in PANC-1 cells treated with AM251 (5 μM) and XCT790 (2.5 μM) for 16 h (Fig. 5C). Preincubation with either drug led to an increase in mitochondrial mass (Fig 5C, left panel) and marked $\Delta\psi_m$ depolarization (Fig. 5C, middle panel). Normalization of $\Delta\psi_m$ values with those of Mitotracker Green demonstrated that both AM251 and XCT790 treatments caused a significant $\Delta\psi_m$ depolarization, which was associated with ERRα protein destabilization (Fig. 5C, bars).

Mitochondrial mass is controlled through biogenesis, degradation, or both processes (Michel et al., 2012). To further examine mitochondrial dyfunction in response to AM251, we compared the expression levels of mitochondrial proteins in the absence or presence of leupeptin and NH_4Cl, two known lysosomal inhibitors. Western blot analysis demonstrated that the expression of COXII and COXIII subunits, cytochrome c and VDAC/porin were unaffected in serum-depleted cells treated or not with leupeptin and NH_4Cl for 5 h (Fig. 5D). However, there was higher expression of VDAC/porin in AM251-treated cells when compared to vehicle controls while the level of COXII and COXIII subunits expression remained constant. Taken together, these data indicate that AM251 induces alterations to both mitochondrial mass and bioenergetics via depletion of ERRα.

We further investigated the possibility that AM251 and XCT790 negatively affected mitochondrial integrity. Treatment of PANC-1 cells with AM251 resulted in the retention of cytochrome c in the mitochondrial compartment whereas a small, but detectable amount of cytochrome c was present in the cytosolic fraction of XCT790-treated cells (Fig. 5E). Neither AM251 nor XCT790 treatment of PANC-1 cells resulted in poly-(ADP-ribose) polymerase-1 cleavage, a process known to occur during apoptosis (Soldani and Scovassi, 2002) (Supplemental Fig. 3). From these data, we conclude that the loss in ERRα protein by AM251 and related biarypyrazole compounds was not accompanied by loss in cell integrity.

Molecular Pharmacology Fast Forward. Published on October 12, 2012 as DOI: 10.1124/mol.112.082651
This article has not been copyedited and formatted. The final version may differ from this version.

Discussion

The nuclear receptor ERRα has important modulatory roles in numerous aspects of energy metabolism, including fatty acid oxidation, glucose metabolism and mitochondrial biogenesis (Ariazi and Jordan, 2006; Villena and Kralli, 2008; Giguère 2008). Therefore, synthetic inverse agonists targeting ERRα may be useful in the treatment of metabolic diseases as well as cancer. Recently, we have shown that AM251 promotes cellular degradation of ERRα protein (Fiori et al., 2011). In the current study, a variety of approaches were used to detect DNA-binding properties, native oligomeric protein complexes, and posttranslational modifications that are known mechanisms for the destabilization and proteolytic degradation of ERRα. We provide novel evidence that AM251 and related biarylpyrazole compounds induce proteasomal degradation of ERRα via posttranslational modifications, and that such degradation subsequently alters mitochondrial function.

Our previous work showed that AM251 displays affinity and specificity for the ligand-binding domain of ERRα, which translated into selective reduction in ERRα protein levels without an effect on its mRNA levels (Fiori et al., 2011). In this study, the destabilization of ERRα by compounds structurally related to AM251 displayed a signature appropriate for this class of drugs. Interestingly, these effects appeared to be cell type-specific as AM251, rimonabant and SLV419 all promoted proteolytic degradation of ERRα in PANC-1 and ES-2 cells but not in the HepG2 cell line. Moreover, no alterations were found in protein levels of ERRγ or that of the co-activator PGC-1, regardless of cell type. However, a marked depletion in ERRα was observed in all cell lines upon exposure to the potent ERRα-specific inverse agonist XCT790. These results, which suggest a model for cell type-specific control of ERRα stability by biarylpyrazole compounds, are supported by findings in ERRα knockout mice, wherein gene induction was strongly dependent on the tissue type (Huss et al., 2004). Alternatively, the selective reduction of ERRα levels in different cell types might fine-tune ERRα signaling, for example, to modulate osteoblastic and adipogenic programs (Ijichi et al., 2007; Delhon et al., 2009). These

Molecular Pharmacology Fast Forward. Published on October 12, 2012 as DOI: 10.1124/mol.112.082651
This article has not been copyedited and formatted. The final version may differ from this version.

findings highlight the complexity and selectivity of ERRα metabolic regulation and suggest the involvement of additional players in the ERRα proteolytic pathway, for example, activation of the calpain proteases and the ubiquitin-proteasome complex.

In order to elucidate whether AM251-induced ERRα loss occurs through decreased protein synthesis and/or increase in proteasomal activity, specific inhibitors of each process were used. The rate of ERRα depletion by AM251 was significantly slower than that elicited by the protein synthesis inhibitor, cycloheximide, indicating that AM251 is likely to act through reduction of protein stability instead of impacting ERRα mRNA translation. Treatment with the proteasomal inhibitor MG132 abrogated AM251-induced ERRα loss, implying participation of the proteasome system. Moreover, there was accumulation of ERRα within the nucleus as a multimeric complex whose DNA binding ability was maintained in the presence of AM251, albeit to a lesser degree due to the depletion of the complex (Fig. 3). The lack of protection against the loss of ERRα in AM251-treated cells that were preincubated with leptomycin B (a CRM1 nuclear export inhibitor) implies that a nuclear proteasome complex is involved in ERRα destabilization by AM251 and related compounds.

Proteasomal degradation typically involves posttranslational modifications of target proteins. ERRα has been shown to undergo numerous modifications including phosphorylation (Sladek et al., 1997; Lu et al., 2011), SUMOylation (Vu et al., 2007; Tremblay et al., 2008), ubiquitination (Ren et al., 2011) and acetylation (Wilson et al., 2010), many of which alter its transcriptional activity. In the current study, AM251 significantly increased SUMOylation of ERRα by SUMO-2,3 (Fig. 4B), a posttranslational modification associated with enhanced protein turnover (Miteva et al., 2010; Manente et al., 2011; Shimshon et al., 2011). Consistent with these findings, protein modifications with SUMO-2,3 have been associated with increased nuclear degradation (Anderson et al., 2012). Previous mutagenesis studies have identified the critical importance of residues Lys-14 and Lys-403 for ERRα SUMOylation (Vu et al., 2007; Tremblay et al., 2008) and found this modification to also occur *in vivo* (Tremblay et al., 2008). SUMOylation has previously been linked to either the promotion (Manente et al., 2011) or inhibition

Molecular Pharmacology Fast Forward. Published on October 12, 2012 as DOI: 10.1124/mol.112.082651
This article has not been copyedited and formatted. The final version may differ from this version.

(Anderson et al., 2012; Sharma et al., 2010) of protein ubiquitination. Despite ERRα being a target of ubiquitination by the E3 ligase Parkin (Ren et al., 2010), our preliminary findings failed to show any significant induction of ERRα ubiquitination by AM251 (data not shown).

Phosphorylation on Ser-19 enhances SUMOylation of ERRα on Lys-14 by SUMO2 (Vu et al., 2007; Tremblay et al., 2008). Since PKCε is a known ERRα kinase (Lu et al., 2011), we next sought to determine if AM251 alters PKC activity. Herein, the demonstration that phorbol ester stimulation can induce ERRα degradation paralleled the action of AM251. Similar with phorbol esters, AM251 also exhibited increased potency toward phosphorylation of an *in vivo* PKC substrate. This may support a role for PKC in triggering phosphorylation-dependent SUMOylation and proteasomal degradation of nuclear ERRα by biarylpyrazole compounds. Moreover, the extent of ERRα phosphorylation could also influence subsequent posttranslational modification of this nuclear receptor, thereby altering the stability of ERRα-containing protein complexes. However, no differences were observed between AM251- and vehicle-treated cells in this respect (Fig. 3B and C). Nuclear extracts were resolved by NativePAGE gel electrophoresis and a single 220-kDa complex was detected in both experimental conditions. In addition, the free monomeric form of ERRα did not exist, and no changes in these parameters were observed upon cell treatment. Although ERRγ, PGC-1 and RIP140 have been found to interact with ERRα, our data indicate that they are not integral members of the endogenous, nuclear ERRα-containing complex. In support of our findings, SUMOylation has no effect on either DNA-binding properties or coactivator recruitment to ERRα (Tremblay et al., 2008). A major effort is currently underway in our laboratory to identify the components of the 220-kDa complex.

Given the critical importance of ERRα in regulating expression of numerous mitochondrial genes (Eichner and Giguère, 2011), we hypothesized that AM251 would subsequently alter mitochondrial function through downregulation of this orphan nuclear receptor. Recent findings have indicated that treatment with the AM251 analog, rimonabant, increased hepatic mitochondrial respiration in rats fed a high-fat diet (Flamment et al., 2009). However, no differences were observed in the quantity of

mitochondrial DNA and the citrate synthase activity. The increase in mitochondrial activity would be expected to increase energy supply, but there was a reduction in ATP synthase activity, consistent with an increase in mitochondrial proton leak (Flamment et al., 2009). Here, we found that treatment with AM251 or siRNA-mediated ERRα silencing exerted negative effects on mitochondrial staining with Mitotracker Red CMXRos. Different hypotheses may explain changes in mitochondrial function: 1) both approaches may interfere with mitochondrial electron transport; 2) mitochondrial activity may be impaired via depletion of NADH; or 3) the mitochondrial permeability transition pore complex may be compromised. It should also be noted that TMRM and mitotracker green assays were also performed and indicated a clear mitochondrial dysfunction in response to AM251 or XCT790 despite increased mitochondrial biogenesis. Moreover, our previous report found that AM251 decreased mRNA level of an important mitochondrial gene, *PDK4* (Fiori et al., 2011). Our observations, together with a recent investigation by Michel and colleagues (Michel et al., 2012), provide examples of a putative retrograde response that enables cells to adapt to impaired mitochondrial activity.

In summary, we have demonstrated that the biarylpyrazole class of compounds reduces ERRα protein stability in association with altered mitochondrial dysfunction. We propose a molecular mechanism that contributes to ERRα degradation via increased PKC activity leading to SUMOylation and subsequent nuclear proteasomal degradation, which, in turn, leads to alterations in genes critical to mitochondrial biogenesis and function. The impairment of metabolic function for ERRα combined with recent reports of the significant effects of AM251 and rimonabant on GPR55, GABA receptors, and μ-opioid receptors (Sharir and Abood, 2010; Baur et al., 2012; Seely eta al., 2012), are suggestive of drugs that in fact display significant off-target effects. Therefore, the findings demonstrated herein may aid in the optimization of future therapeutics aimed at treating metabolic diseases with minimal side effects.

Molecular Pharmacology Fast Forward. Published on October 12, 2012 as DOI: 10.1124/mol.112.082651
This article has not been copyedited and formatted. The final version may differ from this version.

Acknowledgements

We wish to thank Sutapa Kole for her expert technical assistance. We also thank J.F. McElroy for providing rimonabant and SLV319.

Authorship Contributions

Participated in research design: Krzysik-Walker, González-Mariscal, Scheibye-Knudsen, Bernier.

Conducted experiments: Krzysik-Walker, González-Mariscal, Scheibye-Knudsen, Indig.

Contributed new reagents or analytical tools: Scheibye-Knudsen.

Performed data analysis: Krzysik-Walker, González-Mariscal, Scheibye-Knudsen, Indig, Bernier.

Wrote or contributed to the writing of the manuscript: Krzysik-Walker, Bernier.

Molecular Pharmacology Fast Forward. Published on October 12, 2012 as DOI: 10.1124/mol.112.082651
This article has not been copyedited and formatted. The final version may differ from this version.

References

Anderson DD, Eom JY, and Stover PJ (2012) Competition between sumoylation and ubiquitylation of serine hydroxymethyltransferase 1 determines its nuclear localization and its accumulation in the nucleus. *J Biol Chem* **287:**4790−4799.

Ariazi EA and Jordan VC (2006) Estrogen-related receptors as emerging targets in cancer and metabolic disorders. *Curr Top Med Chem* **6:**203–215.

Barry JB and Giguère V (2005) Epidermal growth factor-induced signaling in breast cancer cells results in selective target gene activation by orphan nuclear receptor estrogen-related receptor α. *Cancer Res* **65:**6120–6129.

Baur R, Gertsch J, and Sigel E (2012) The cannabinoid CB1 receptor antagonists rimonabant (SR141716) and AM251 directly potentiate GABA(A) receptors. *Br J Pharmacol* **165:**2479-2484.

Delhon I, Gutzwiller S, Morvan F, Rangwala S, Wyder L, Evans G, Studer A, Kneissel M, and Fournier B (2009) Absence of estrogen receptor-related-alpha increases osteoblastic differentiation and cancellous bone mineral density. *Endocrinology* **150:**4463−4472.

Eichner LJ and Giguère V (2011) Estrogen related receptors (ERRs): a new dawn in transcriptional control of mitochondrial gene networks. *Mitochondrion* **11:**544–552.

Fiori JL, Sanghvi M, O'Connell MP, Krzysik-Walker SM, Moaddel R, and Bernier M (2011) The cannabinoid receptor inverse agonist AM251 regulates the expression of the EGF receptor and its ligands via destabilization of oestrogen-related receptor α protein. *Br J Pharmacol* **164:**1026–1040.

Flamment M, Gueguen N, Wetterwald C, Simard G, Malthièry Y, and Ducluzeau PH (2009) Effects of the cannabinoid CB1 antagonist rimonabant on hepatic mitochondrial function in rats fed a high-fat diet. *Am J Physiol Endocrinol Metab* **297:**E1162-E1170.

Giguère V (2008) Transcriptional control of energy homeostasis by the estrogen-related receptors. *Endocr Rev* **29**:677–696.

Molecular Pharmacology Fast Forward. Published on October 12, 2012 as DOI: 10.1124/mol.112.082651
This article has not been copyedited and formatted. The final version may differ from this version.

Henstridge CM, Balenga NA, Ford LA, Ross RA, Waldhoer M, and Irving AJ (2009) The GPR55 ligand L-alpha-lysophosphatidylinositol promotes RhoA-dependent Ca2+ signaling and NFAT activation. *FASEB J* **23:**183–193.

Horard B, Castet A, Bardet PL, Laudet V, Cavailles V, and Vanacker JM (2004) Dimerization is required for transactivation by estrogen-receptor-related (ERR) orphan receptors: evidence from amphioxus ERR. *J Mol Endocrinol* **33:**493–509.

Huss JM, Torra IP, Staels B, Giguère V, and Kelly DP (2004) Estrogen-related receptor alpha directs peroxisome proliferator-activated receptor alpha signaling in the transcriptional control of energy metabolism in cardiac and skeletal muscle. *Mol Cell Biol* **24**:9079–9091.

Ijichi N, Ikeda K, Horie-Inoue K, Yagi K, Okazaki Y, and Inoue S (2007) Estrogen-related receptor alpha modulates the expression of adipogenesis-related genes during adipocyte differentiation. *Biochem Biophys Res Commun* **358:**813−818.

Jin K, Xie L, Kim SH, Parmentier-Batteur S, Sun Y, Mao XO, Childs J, and Greenberg DA (2004) Defective adult neurogenesis in CB1 cannabinoid receptor knockout mice. *Mol Pharmacol* **66:**204–208.

Kallen J, Schlaeppi JM, Bitsch F, Filipuzzi I, Schilb A, Riou V, Graham A, Strauss A, Geiser M, and Fournier B (2004) Evidence for ligand-independent transcriptional activation of the human estrogen-related receptor alpha (ERRα): crystal structure of ERRα ligand binding domain in complex with peroxisome proliferator-activated receptor coactivator-1α. *J Biol Chem* **279:**49330–49337.

Kapur A, Zhao P, Sharir H, Bai Y, Caron MG, Barak LS, and Abood ME (2009) Atypical responsiveness of the orphan receptor GPR55 to cannabinoid ligands. *J Biol Chem* **284:**29817–29827.

Lanvin O, Bianco S, Kersual N, Chalbos D and Vanacker JM (2007) Potentiation of ICI182,780 (Fulvestrant)-induced estrogen receptor-alpha degradation by the estrogen receptor-related receptor-alpha inverse agonist XCT790. *J Biol Chem* **282:**28328–28334.

Lu N, Wang W, Liu J and Wong CW (2011) Protein kinase C epsilon affects mitochondrial function

through estrogen-related receptor alpha. *Cell Signal* **23**:1473–1478.

Luo J, Sladek R, Carrier J, Bader JA, Richard D, and Giguère V (2003) Reduced fat mass in mice lacking orphan nuclear receptor estrogen-related receptor alpha. *Mol Cell Biol* **23:**7947–7956.

Manente AG, Pinton G, Tavian D, Lopez-Rodas G, Brunelli E, and Moro L (2011) Coordinated sumoylation and ubiquitination modulate EGF induced EGR1 expression and stability. *PLoS One* **6:**e25676.

Michel S, Wanet A, De Pauw A, Rommelaere G, Arnould T, and Renard P (2012) Crosstalk between mitochondrial (dys)function and mitochondrial abundance. *J Cell Physiol* **227:**2297–2310.

Miteva M, Keusekotten K, Hofmann K, Praefcke GJ, and Dohmen RJ (2010) Sumoylation as a signal for polyubiquitylation and proteasomal degradation. *Subcell Biochem* **54:**195−214.

Moreno-Navarrete JM, Catalán V, Whyte L, Díaz-Arteaga A, Vázquez-Martínez R, Rotellar F, Guzmán R, Gómez-Ambrosi J, Pulido MR, Russell WR, Imbernón M, Ross RA, Malagón MM, Dieguez C, Fernández-Real JM, Frühbeck G, and Nogueiras R (2012) The L-α-lysophosphatidylinositol/GPR55 system and its potential role in human obesity. *Diabetes* **61:**281–291.

Padwal RS and Majumdar SR (2007) Drug treatments for obesity: orlistat, sibutramine, and rimonabant. *Lancet* **369:**71–77.

Pegorini S, Zani A, Braida D, Guerini-Rocco C, and Sala M (2006) Vanilloid VR1 receptor is involved in rimonabant-induced neuroprotection. *Br J Pharmacol* **147:**552–559.

Raffa RB and Ward SJ (2012) CB□-independent mechanisms of Δ□-THCV, AM251 and SR141716 (rimonabant). *J Clin Pharm Ther* **37:**260–265.

Ravinet Trillou C, Delgorge C, Menet C, Arnone M, and Soubrie P (2004) CB1 cannabinoid receptor knockout in mice leads to leanness, resistance to diet-induced obesity and enhanced leptin sensitivity. *Int J Obes Relat Metab Disord* **28:**640–648.

Ren Y, Jiang H, Ma D, Nakaso K, and Feng J (2011) Parkin degrades estrogen-related receptors to limit the expression of monoamine oxidases. *Hum Mol Genet* **20:**1074−1083.

Schreiber SN, Emter R, Hock MB, Knutti D, Cardenas J, Podvinec M, Oakeley EJ, and Kralli A (2004)

The estrogen-related receptor alpha (ERRα) functions in PPARgamma coactivator 1alpha (PGC-1α)-induced mitochondrial biogenesis. *Proc Natl Acad Sci USA* **101:**6472–6477.

Seely KA, Brents LK, Franks LN, Rajasekaran M, Zimmerman SM, Fantegrossi WE, and Prather PL (2012) AM-251 and rimonabant act as direct antagonists at mu-opioid receptors: Implications for opioid/cannabinoid interaction studies. *Neuropharmacology* **63:**905-915.

Seppet E, Gruno M, Peetsalu A, Gizatullina Z, Nguyen HP, Vielhaber S, Wussling MH, Trumbeckaite S, Arandarcikaite O, Jerzembeck D, Sonnabend M, Jegorov K, Zierz S, Striggow F, and Gellerich FN (2009) Mitochondria and energetic depression in cell pathophysiology. *Int J Mol Sci* **10:**2252–2303.

Sharir H and Abood ME (2010) Pharmacological characterization of GPR55, a putative cannabinoid receptor. *Pharmacol Ther* **126:**301−313.

Sharma P, Murillas R, Zhang H, and Kuehn MR (2010) N4BP1 is a newly identified nucleolar protein that undergoes SUMO-regulated polyubiquitylation and proteasomal turnover at promyelocytic leukemia nuclear bodies. *J Cell Sci* **123**:1227−1234.

Shimshon L, Michaeli A, Hadar R, Nutt SL, David Y, Navon A, Waisman A, and Tirosh B (2011) SUMOylation of Blimp-1 promotes its proteasomal degradation. *FEBS Lett* **585:**2405−2409.

Sladek R, Bader JA, and Giguère V (1997) The orphan nuclear receptor estrogen-related receptor alpha is a transcriptional regulator of the human medium-chain acyl coenzyme A dehydrogenase gene. *Mol Cell Biol* **17:**5400–5409.

Soldani C and Scovassi AI (2002) Poly(ADP-ribose) polymerase-1 cleavage during apoptosis: an update. *Apoptosis* **7:**321–328.

Swamy M, Siegers GM, Minguet S, Wollscheid B, and Schamel WW (2006) Blue native polyacrylamide gel electrophoresis (BN-PAGE) for the identification and analysis of multiprotein complexes. *Sci STKE* **2006:**pl4.

Tremblay AM, Wilson BJ, Yang XJ, and Giguère V (2008) Phosphorylation-dependent sumoylation regulates estrogen-related receptor-alpha and -gamma transcriptional activity through a synergy control motif. *Mol Endocrinol* **22:**570−584.

Villena JA and Kralli A (2008) ERRalpha: a metabolic function for the oldest orphan. *Trends Endocrinol Metab* **19:**269–276.

Vu EH, Kraus RJ, and Mertz JE (2007) Phosphorylation-dependent sumoylation of estrogen-related receptor alpha1. *Biochemistry* **46:**9795−9804.

Waldeck-Weiermair M, Zoratti C, Osibow K, Balenga N, Goessnitzer E, Waldhoer M, Malli R, and Graier WF (2008) Integrin clustering enables anandamide-induced Ca2+ signaling in endothelial cells via GPR55 by protection against CB1-receptor-triggered repression. *J Cell Sci* **121:**1704−1717.

Wiley JL, Selley DE, Wang P, Kottani R, Gadthula S, and Mahadeven A (2012) 3-Substituted pyrazole analogs of the cannabinoid type 1 (CB□) receptor antagonist rimonabant: cannabinoid agonist-like effects in mice via non-CB□, non-CB□ mechanism. *J Pharmacol Exp Ther* **340:**433−444.

Wilson BJ, Tremblay AM, Deblois G, Sylvain-Drolet G, and Giguère V (2010) An acetylation switch modulates the transcriptional activity of estrogen-related receptor alpha. *Mol Endocrinol* **24**:1349−1358.

Wu KK (2006) Analysis of protein-DNA binding by streptavidin-agarose pulldown. *Methods Mol Biol* **338:**281–290.

Xie W, Hong H, Yang NN, Lin RJ, Simon CM, Stallcup MR, and Evans RM (1999) Constitutive activation of transcription and binding of coactivator by estrogen-related receptors 1 and 2. *Mol Endocrinol* **13:**2151–2162.

Zhang Z and Teng CT (2000) Estrogen receptor-related receptor alpha 1 interacts with coactivator and constitutively activates the estrogen response elements of the human lactoferrin gene. *J Biol Chem* **275:**20837–20846.

Footnotes

This research was supported entirely by the Intramural Research Program of the National Institutes of Health (NIH), National Institute on Aging.

Address Correspondence to: Michel Bernier, Laboratory of Clinical Investigation, Biomedical Research Center, National Institute on Aging, NIH, 251 Bayview Boulevard, Suite 100, Baltimore, MD 21224.

Email: Bernierm@mail.nih.gov

Molecular Pharmacology Fast Forward. Published on October 12, 2012 as DOI: 10.1124/mol.112.082651
This article has not been copyedited and formatted. The final version may differ from this version.

Figure Legends

Fig. 1. Biarylpyrazole compounds destabilize ERRα protein in PANC-1 cells. A, Serum-depleted PANC-1 cells were incubated either with vehicle (DMSO) or 5 μM of the biarylpyrazole compounds, AM251, rimonabant or SLV319 for 16 h. The ERRα inverse agonist XCT790 (2.5 μM) was included as a positive control. B, PANC-1 cells were incubated with the indicated concentrations of the biarylpyrazole compounds for 16 h. Total cellular extracts were prepared and analyzed by immunoblotting with antibodies against ERRα, ERRγ, and Hsp90, with the latter serving as a loading control. The relative expression of ERRα was determined by densitometry and normalized to Hsp90. Bars represent means ± SEM from 4-6 independent experiments (panel A) or means ± range of two sets of dishes (panel B). The migration of molecular-mass markers (values in kilodaltons) is shown on the left of immunoblots. ***, $P < 0.001$ *vs.* DMSO-treated cells.

Fig. 2. AM251-mediated proteasomal degradation of nuclear ERRα. A, Serum-depleted PANC-1 cells were treated in the absence or presence of 10 μg/ml cycloheximide (CHX) or AM251 (5 μM) for the indicated periods of time. Total cellular extracts were prepared and analyzed by immunoblotting with antibodies against ERRα and PGC-1. GAPDH was used as a loading control. The relative expression of ERRα was determined by densitometry and normalized to GAPDH. Data represent means ± range of two sets of dishes. B, Serum-depleted PANC-1 cells were treated with MG132 (10 μM) for 1 h followed by the addition either of CHX (10 μg/ml) or AM251 (5 μM) for 15 h. Western blotting was performed as in (A). Left panel, representative blots; right panel, bars represent means ± range of two sets of dishes. C, Serum-depleted PANC-1 cells were treated with MG132 (10 μM) for 1 h followed by the addition of vehicle (DMSO, 0.1%) or AM251 (5 μM) for 15 h. Nuclear (N) and cytosolic (C) fractions were prepared and analyzed by immunoblotting with antibodies against ERRα and Hsp70, which was used as a loading control (upper panels). The membranes were then reprobed with antibodies specific for the nuclear

Molecular Pharmacology Fast Forward. Published on October 12, 2012 as DOI: 10.1124/mol.112.082651
This article has not been copyedited and formatted. The final version may differ from this version.

marker BRG-1 and cytoplasmic marker IκBα (lower panels). Similar results were obtained in a second independent experiment.

Fig. 3. DNA-binding properties of a nuclear multimeric protein complex encompassing ERRα. A, Control and MG132-treated PANC-1 cells were incubated with AM251 (5 μM) or XCT790 (2.5 μM) for 16 h. Nuclear extracts were prepared and DNA binding activity of ERRα was determined as described in "*Materials and Methods*". Nuclear extracts were incubated with agarose-bound oligonucleotide probe containing the wild-type (wt) ERRE consensus sequence (lanes 2-7) or the same probe mutated (mut) at the ERRE site (lanes 1, 8). Bound ERRα (lanes 1-7) and unbound ERRα from the mut oligonucleotide incubation (mut-NA, lane 8) were immunoblotted with antibodies against ERRα. Identical results were obtained in a second independent experiment. B and C, Nuclear extracts from panel A were also resolved by NativePAGE, enabling the separation of native ERRα-containing multiprotein complexes (B), and complexes expressing ERRγ, PGC-1 and RIP140 (C). Similar results were obtained in a second independent experiment. The migration of molecular-mass markers (values in kilodaltons) is shown on the left of immunoblots.

Fig. 4. AM251 induces posttranslational modifications of ERRα and its targeting to the nuclear proteasome. A, Serum-starved PANC-1 cells were pretreated either with MG132 (10 μM), leptomycin B (5 nM), or the combination MG132 + leptomycin B for 1h followed by the addition of vehicle (DMSO, 0.1%), AM251 (5 μM) or XCT790 (2.5 μM) for 16 h. Cell lysates were analyzed by Western blot for the detection of ERRα and Hsp90. Bars represent means ± SEM (n=4) of two independent experiments, each performed with two dishes per group. B, PANC-1 cells were serum-depleted and then treated with or without AM251 for 16 h. Nuclear extracts were prepared, subjected to immunoprecipitation (IP) with anti-ERRα and then immunoblotted for SUMO-2,3 (*upper panel*). Reciprocal immunoprecipitation was carried out whereby anti-SUMO-2,3 immunoprecipitates were analyzed by Western blot with anti-ERRα

Molecular Pharmacology Fast Forward. Published on October 12, 2012 as DOI: 10.1124/mol.112.082651
This article has not been copyedited and formatted. The final version may differ from this version.

(*middle panel*). Control immunoprecipitation (crtl) was performed with protein G beads alone. Five percent of input (before IP) was loaded on the gel (*bottom panel*). Blots from a representative experiment are shown. Bars represent the immunoblot signals normalized to input. C, Serum-depleted PANC-1 cells were treated with PMA (10 nM) or AM251 for 7 h and then processed for Western blotting. Results are expressed as means ± SEM of 3 experiments, each performed in duplicate dishes. D, Total RNA from PANC-1 cells treated with vehicle (DMSO, 0.1%), PMA (10 nM) or AM251 (5 μM) for 7 h was extracted and analyzed for ERRα and 18S by quantitative real-time PCR. Bars represent means ± SEM of 2 independent experiments, each performed in duplicate dishes. E, Serum-depleted PANC-1 cells were treated with PMA or AM251 for 30 min followed by immunoblot analysis with antibodies against phosphorylated MARCKS and GAPDH, which served as a normalization control. Data represent means ± SEM (n=3) of a representative experiment. Similar results were obtained in a second independent experiment. Different letters (a, b, c) indicate significant differences at $P < 0.05$.

Fig. 5. ERRα depletion alters mitochondrial biogenesis and membrane potential. A, Serum-depleted PANC-1 cells were treated with vehicle (DMSO) or AM251 (5 μM) for 16 h. Cells were incubated with MitoTracker Red CMXRos, rinsed with PBS, fixed, permeabilized, and then cell nuclei were counterstained with 4',6-diamidino-2-phenylindole (DAPI; *blue*). Cells were examined by fluorescence microscopy, as described in Material and Methods. B, PANC-1 cells were transfected with a control, non-silencing siRNA or ERRα siRNA for 48 h followed by MitoTracker Red CMXRos staining. Mitochondria that have lost membrane potential are no longer visible after MitoTracker staining of the cells. Scale bar, 10 μm. C, Serum-depleted PANC-1 cells were treated with vehicle (DMSO; *red*), AM251 (5 μM; *blue*) or XCT790 (2.5 μM; *green*) for 16 h. Cells were analyzed by flow cytometry after staining with Mitotracker Green and TMRM to differentiate intact mitochondria from cellular debris and determine $\Delta\psi m$, respectively. Left panel, representative Mitotracker-Green flow cytometric histograms (FITC channel); middle panel, representative TMRM flow cytometric histograms (red fluorescence); right

Molecular Pharmacology Fast Forward. Published on October 12, 2012 as DOI: 10.1124/mol.112.082651
This article has not been copyedited and formatted. The final version may differ from this version.

panel, graphic representation of the pooled experiments. Relative $\Delta\psi m$ is expressed as percentage of the mean fluorescence intensity of the Mitotracker Green-positive cell population, which was set at 100% in DMSO control. Bars represent means ± SD of 2 independent experiments each performed in duplicate dishes (n=4). In each analysis, 10 000 events were recorded. X-axis x 10^3. D, Determination of mitochondrial protein expression levels in the presence and absence of lysosomal inhibitors, NH_4^+Cl/leupeptin, in control and AM251-treated PANC-1 cells. Serum-depleted cells were treated with DMSO or AM251 (5 μM) for 12 h followed by the addition of NH_4^+Cl/leupeptin for the next 4 h. Total cell extracts were analyzed by immunoblotting with the indicated antibodies, and Hsp90 was used as a loading control. Top panel, representative immunoblots; bottom panel, densitometry of VDAC/porin and ERRα followed by normalization with Hsp90. Data represent means ± SEM of 3 separate experiments, each performed in duplicate. Filled bars, VDAC; hatched bars, ERRα. * $P < 0.05$. E, Cytosolic (C) and mitochondrial (M) fractions were prepared from PANC-1 cells treated either with DMSO (0.1%), AM251 (5 μM) or XCT790 (2.5 μM) for 16 h. Immunoblotting was performed with the indicated antibodies. Similar results were obtained in a separate experiment.

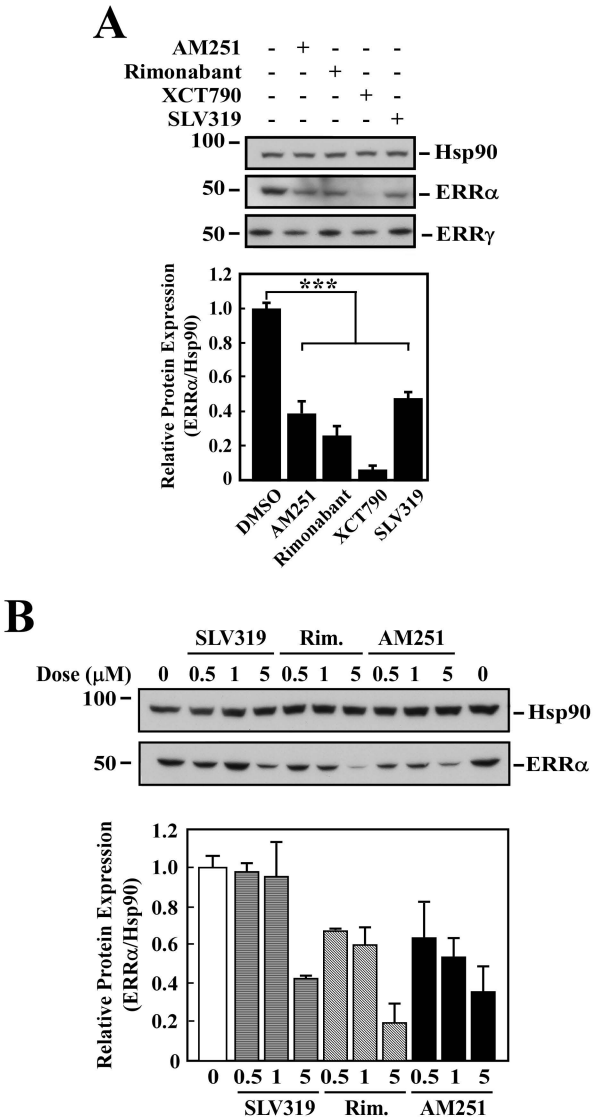
A
AM251 - + - - -
Rimonabant - - + - -
XCT790 - - - + -
SLV319 - - - - +
100
50
50
Hsp90
ERRα
ERRγ
Relative Protein Expression (ERRα/Hsp90)
1.2
1.0
0.8
0.6
0.4
0.2
0
***
DMSO
AM251
Rimonabant
XCT790
SLV319
B
SLV319
Rim.
AM251
Dose (μM) 0 0.5 1 5 0.5 1 5 0.5 1 5 0
100
50
Hsp90
ERRα
Relative Protein Expression (ERRα/Hsp90)
1.2
1.0
0.8
0.6
0.4
0.2
0
0 0.5 1 5 0.5 1 5 0.5 1 5
SLV319
Rim.
AM251

Figure 1

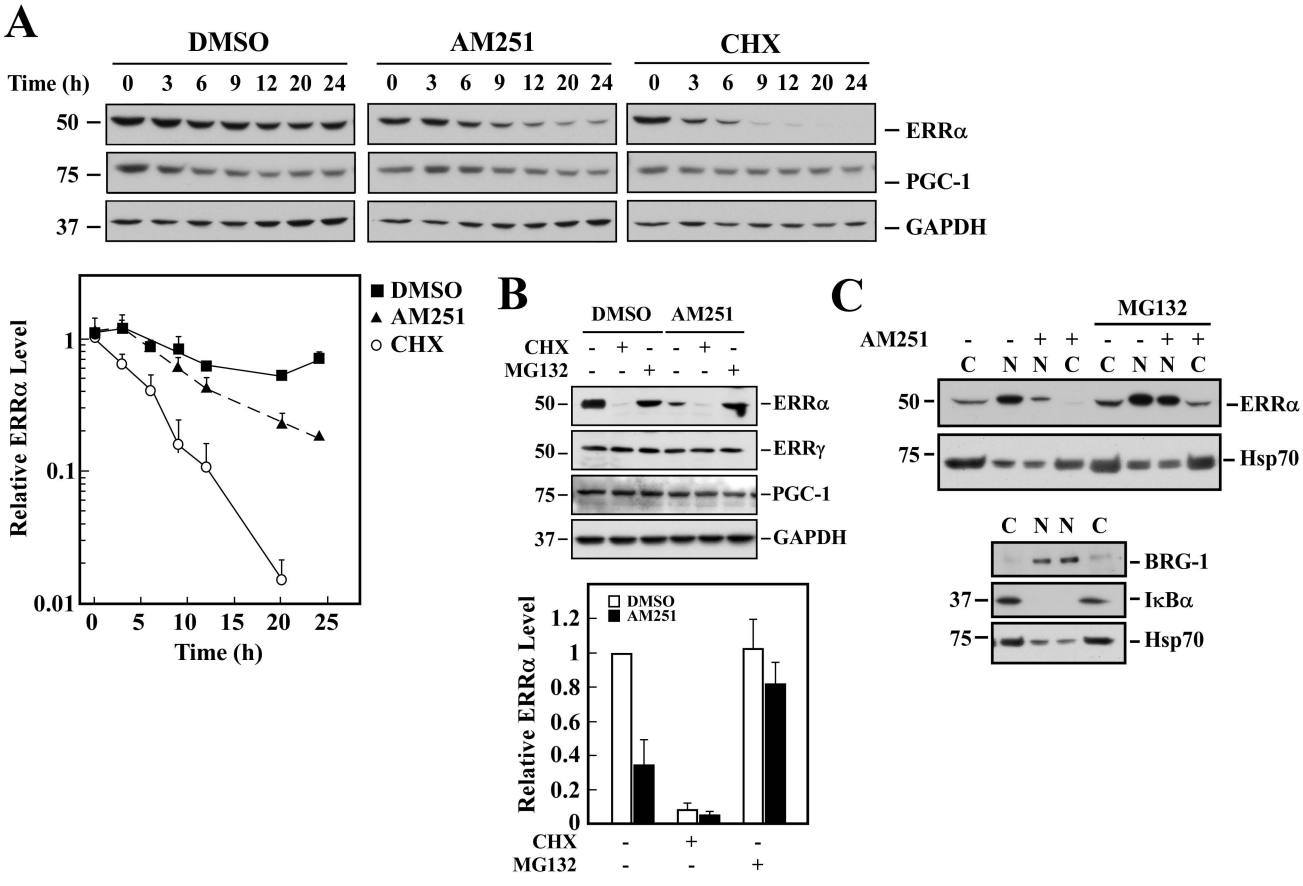
A
DMSO
AM251
CHX
Time (h)
0 3 6 9 12 20 24
50
75
37
ERRα
PGC-1
GAPDH
Relative ERRα Level
DMSO
AM251
CHX
Time (h)
B
DMSO AM251
CHX
MG132
ERRγ
C
MG132
AM251
C N N C C N N C
BRG-1
IκBα
Hsp70

Figure 2

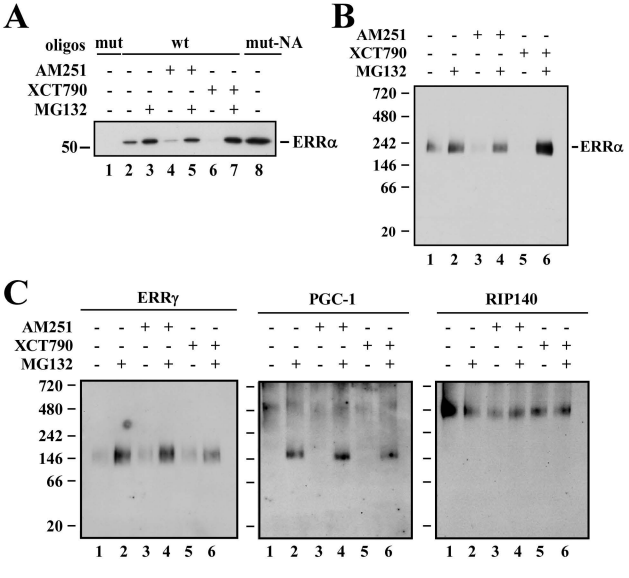
A
oligos mut wt mut-NA
AM251 - - - + + - - -
XCT790 - - - - - + + -
MG132 - - + - + - + -
50
ERRα
1 2 3 4 5 6 7 8
B
AM251 - - + + - -
XCT790 - - - - + +
MG132 - + - + - +
720
480
242
146
66
20
ERRα
1 2 3 4 5 6
C
ERRγ
PGC-1
RIP140
AM251 - - + + - -
XCT790 - - - - + +
MG132 - + - + - +
720
480
242
146
66
20
1 2 3 4 5 6

Figure 3

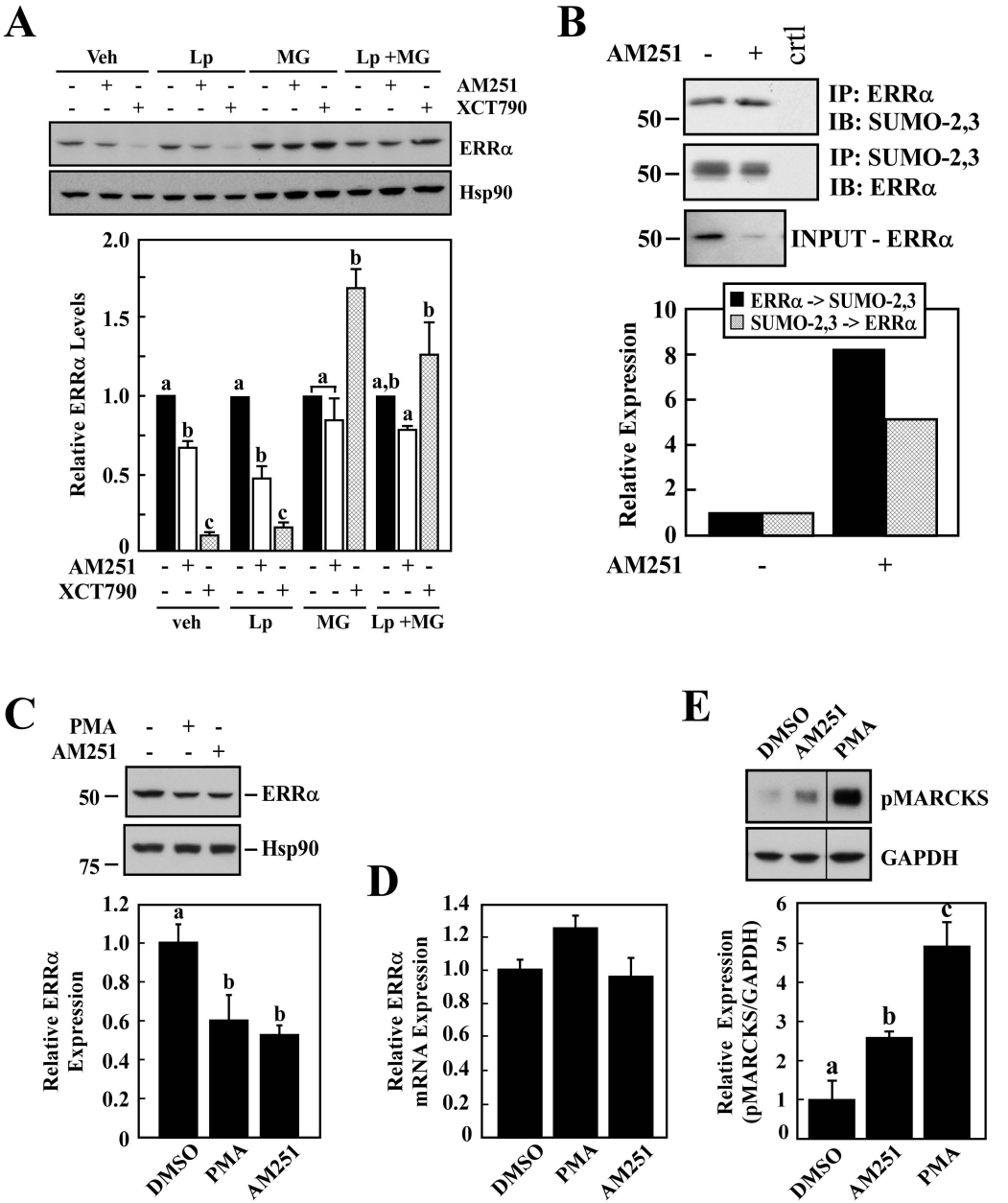
A
Veh
Lp
MG
Lp +MG
AM251
XCT790
ERRα
Hsp90
Relative ERRα Levels
B
AM251
crtl
IP: ERRα
IB: SUMO-2,3
IP: SUMO-2,3
IB: ERRα
INPUT - ERRα
ERRα -> SUMO-2,3
SUMO-2,3 -> ERRα
Relative Expression
C
PMA
AM251
ERRα
Hsp90
Relative ERRα Expression
DMSO
PMA
AM251
D
Relative ERRα mRNA Expression
E
pMARCKS
GAPDH
Relative Expression (pMARCKS/GAPDH)

Figure 4

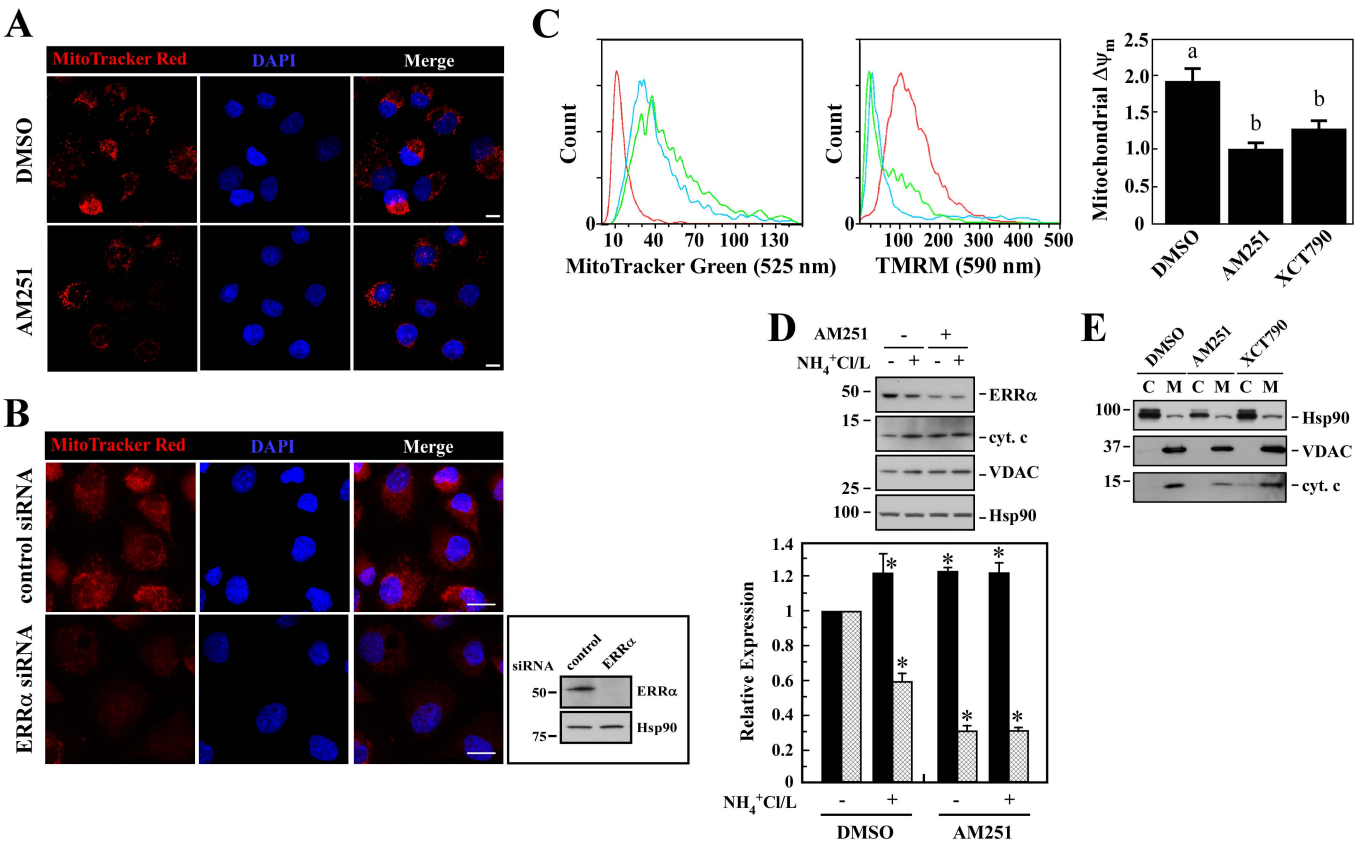
A
MitoTracker Red
DAPI
Merge
DMSO
AM251
B
control siRNA
ERRα siRNA
siRNA
control
ERRα
50
75
ERRα
Hsp90
C
Count
0
10 40 70 100 130
MitoTracker Green (525 nm)
100 200 300 400 500
TMRM (590 nm)
Mitochondrial Δψm
2.5
2.0
1.5
1.0
0.5
0
a
b
b
DMSO
AM251
XCT790
D
AM251
NH4+Cl/L
50
15
25
100
ERRα
cyt. c
VDAC
Hsp90
Relative Expression
1.4
1.2
1
0.8
0.6
0.4
0.2
0
DMSO
AM251
E
DMSO
AM251
XCT790
C M C M C M
100
37
15
Hsp90
VDAC
cyt. c

Figure 5

Supplemental material for Molecular Pharmacology, Ms # 82651

The biarylpyrazole compound AM251 alters mitochondrial physiology via proteolytic degradation of ERRα.

Susan M. Krzysik-Walker, Isabel Gonzalez-Mariscal, Morten Scheibye-Knudsen, Fred E. Indig, and Michel Bernier

Supplemental Figure 1. Biarylpyrazole compounds destabilize ERRα in a cell type-specific manner.

Supplemental Figure 2. Cell type-specific effects of AM251 on mitochondrial membrane potential.

Supplemental Figure 3. Lack of cleavage of PARP-1 by AM251 or XCT790.

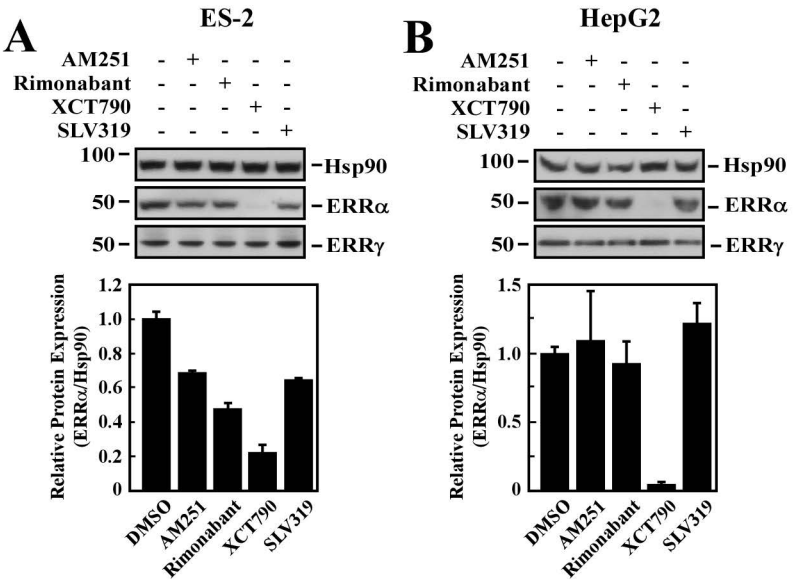

Supplemental Fig. 1. Biarylpyrazole compounds destabilize ERRα in a cell type-specific manner. Serum-depleted ES-2 (A) and HepG2 (B) cells were incubated with either vehicle (DMSO) or 5 μM of AM251, rimonabant or SLV319. The ERRα inverse agonist XCT790 (2.5 μM) was included as a positive control. Total cell extracts were prepared and analyzed by immunoblotting with antibodies against ERRα, ERRγ and Hsp90, the latter serving as a loading control. The relative expression of ERRα was determined by densitometry and normalized to Hsp90. Bars represent means +/- range of two dishes from a single experiment. Comparable results were obtained in a second independent experiment. The migration of molecular-mass markers (values in kilodaltons) is shown on the left of immunoblots.

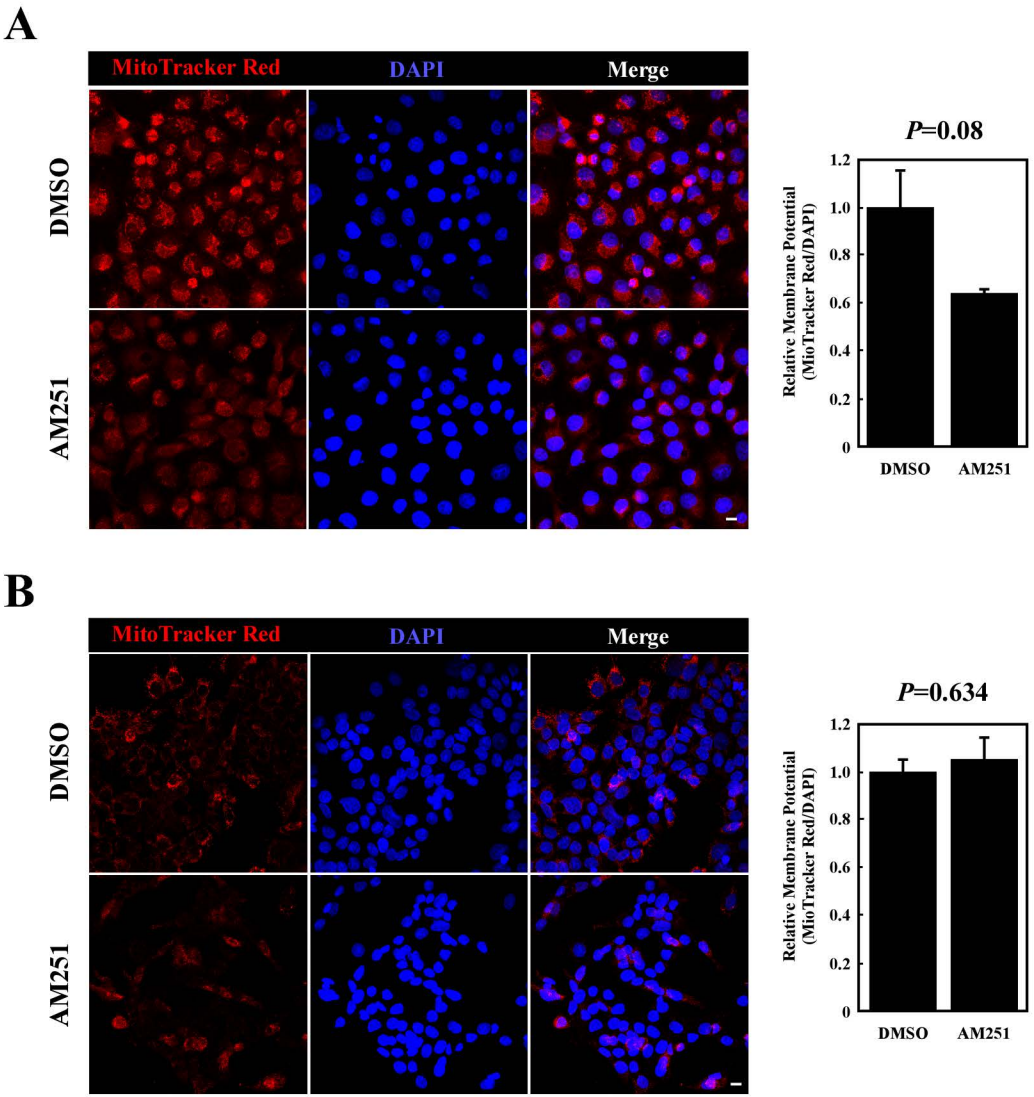

Supplemental Fig. 2. Cell type-specific effects of AM251 on mitochondrial membrane potential. Forty-eight hours after seeding PANC-1 (A) and HepG2 (B) cells into chamber slides, cells in serum-free medium were treated with vehicle (0.1% DMSO) or AM251 (5 μM) for 16 h. The spent medium was replaced with serum-free medium containing 100 nM MitoTracker Red CMXRos for 10 min at 37 ºC. Cells were rinsed in PBS, fixed, permeabilized and then mounted in Prolong Gold antifade medium containing 4',6-diamidino-2-phenylindole (DAPI, blue) to counterstain cell nuclei. Images were captured by confocal microscopy with Z-stack images processed for maximum projection using the Zeiss Zen software. Relative membrane potential was calculated as histogram density of MitoTracker Red CMXRos normalized to DAPI (Bars). Means +/- SD (n=3-4) are presented. Student's t-test was performed to determine significance. Scale bar, 10 μm.

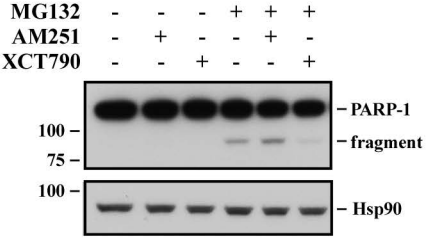

Supplemental Fig. 3. Lack of cleavage of PARP-1 by AM251 or XCT790. Control and MG132-treated PANC-1 cells were incubated with AM251 (5 μM) or XCT790 (2.5 μM) for 16 h. Total cell extracts were immunoblotted with antibodies against PARP-1 and Hsp90, which served as a loading control. Note the weak formation of the 89-kDa fragment of PARP-1 in MG132-treated cells.